Society For Biomaterials

The influence of particle size and static magnetic fields on the uptake of magnetic nanoparticles into three dimensional cell-seeded collagen gel cultures

Emily E. L. Lewis,[1] Hannah W. Child,[1] Andrew Hursthouse,[2] David Stirling,[2] Mark McCully,[1] David Paterson,[1] Margaret Mullin,[3] Catherine C. Berry[1]

[1]Centre for Cell Engineering, University of Glasgow, Glasgow, UK G12 8QQ
[2]School of Science, University of the West of Scotland, Paisley, UK, PA1 2BE
[3]Electron Microscopy Unit, University of Glasgow, Glasgow, UK, G12 8QQ

Received 14 January 2014; revised 18 August 2014; accepted 1 October 2014
Published online 00 Month 2014 in Wiley Online Library (wileyonlinelibrary.com). DOI: 10.1002/jbm.b.33302

Abstract: Over recent decades there has been and continues to be major advances in the imaging, diagnosis and potential treatment of medical conditions, by the use of magnetic nanoparticles. However, to date the majority of cell delivery studies employ a traditional 2D monolayer culture. This article aims to determine the ability of various sized magnetic nanoparticles to penetrate and travel through a cell seeded collagen gel model, in the presence or absence of a magnetic field. Three different sized (100, 200, and 500 nm) nanoparticles were employed in the study. The results showed cell viability was unaffected by the presence of nanoparticles over a 24-h test period. The initial uptake of the 100 nm nanoparticle into the collagen gel structure was superior compared to the larger sized nanoparticles under the influence of a magnetic field and incubated for 24 h. Interestingly, it was the 200 nm nanoparticles, which proved to penetrate the gel furthest, under the influence of a magnetic field, during the initial culture stage after 1-h incubation. © 2014 The Authors. Journal of Biomedical Materials Research Part B: Applied Biomaterials Published by Wiley Periodicals, Inc. J Biomed Mater Res Part B: Appl Biomater 00B: 000–000, 2014.

Key Words: nanotechnology, magnetic nanoparticles, 3D culture, collagen gels

How to cite this article: Lewis EEL, Child HW, Hursthouse A, Stirling D, McCully M, Paterson D, Mullin M, Berry CC. 2014. The influence of particle size and static magnetic fields on the uptake of magnetic nanoparticles into three dimensional cell-seeded collagen gel cultures. J Biomed Mater Res Part B 2014:00B:000–000.

INTRODUCTION

Nanotechnology, in the field of medical science, has led to increased interest in the development and application of nanoparticles (NP).[1] These nanoparticles may be produced from various materials, ranging from metals to polymers; creating different molecular shapes, including rods and spheres.[1,2] Within medical and biological research, nanoparticles have widespread applications, ranging from aiding tissue and cell imaging to delivery of therapeutic molecules.[3,4] The use of magnetic nanoparticles (mNPs) in particular, has led to the simultaneous targeting of a specific disease, imaging the site and delivering the required therapy in medical treatment.[5] Magnetic nanoparticles are composed of a metal core with a biocompatible surface coating.[6] Iron oxide is the most commonly used nanoparticle core metal because it possesses superparamagnetic properties, thus allowing the possibility of remotely controlling the NP location.[7] A further benefit of iron oxide core nanoparticles has been in the treatment of cancer patients. The cancerous tumors are injected with mNPs, which generate heat when they are exposed to a magnetic field thus killing the tumor cells.[8,9]

Almost all biomedical applications are dependent on the uptake of NPs into the cells, which is typically achieved by a process called endocytosis.[10] Endocytosis may be further sub-categorized into either (a) phagocytosis, (b) pinocytosis, or (c) receptor mediated endocytosis, by either clathrin-mediated endocytosis or caveolin-mediated endocytosis.[10,11] The particular endocytosis pathway utilized by the cell is dependent upon the surface chemistry, size, charge, and shape of the NP.[10] A current research drive has focused on increasing the cellular uptake of NPs and studies have shown that applying an external magnetic field enhances cellular uptake of mNPs, as well as the ability to target a diseased site.[5,12] Previous studies have shown the influence of the force from the external magnetic field on mNPs is dependent on the size of the mNP.[13] Therefore, the larger the particle, the greater the influence of the acting force due to the higher

Additional Supporting Information may be found in the online version of this article.
Correspondence to: E. E. L. Lewis; e-mail: e.lewis.1@research.gla.ac.uk

magnetic moment of the NP. This evidence must be balanced against the knowledge that smaller NPs have generally superior tissue accessibility and subsequent cellular uptake.

To date, most research has focused on monolayer cell culture studies, however it was noted these studies do not reflect the *in vivo* environment.[14] Multi-cell-layer studies are a step toward mimicking the 3D architecture of the *in vivo* tissue, and studies using 100 nm NPs indicated that a magnetic field (0.4 T) pulled twice as many particles through as compared to without.[15,16] However, as NPs would need to cross membrane barriers and enter into 3D tissue to be effective, more recent investigations have progressed to the use of cell-seeded scaffolds, such as collagen gels; to recreate three-dimensional (3D) models of cells in a tissue environment.[17] The movement of NPs through these more complex, fibrous networks is far less predictable than movement through liquids such as culture medium, which move at a constant rate proportional to fluid viscosity.[18] The study presented here has investigated the effect of a static magnetic field on mNPs entering a tissue equivalent model. Child et al. recently demonstrated, using a type I collagen gel culture system, an increased mNP (200 nm) uptake in the presence of a magnetic field, as well as a five-order magnitude increase in depth penetration.[17] Previous research has shown a size dependent NP response when a magnetic field was used, thus this study extends this work to investigate the most favorable mNP size in terms of uptake into a 3D tissue equivalent model, in order to optimize potential mNP use in a clinical situation.

EXPERIMENTAL SECTION

Cell culture and collagen gel synthesis

Infinity telomerase-immortalized primary human fibroblasts (h-TERT-BJ1, Clontech Laboratories) were grown in modified Dulbecco's Modified Eagle's Medium (DMEM) (Sigma–Aldrich). The modified DMEM contained 71% DMEM, 17.5% Medium 199 (Sigma–Aldrich), 10% fetal bovine serum (FBS) (Lonza), 0.5% 100 m*M* sodium pyruvate (Life Technologies) and 1% penicillin-streptomycin (PAA Laboratories). Cells were grown until fully confluent and trypsinized ready for use. Gels were prepared using the method previously developed by our group.[17]

The following preparation method was used for making three gels. Quantities were increased depending on how many gels were required for each experiment. Gels were prepared on ice; mixing 0.5 mL of FBS, 0.5 mL 10xDMEM (First Link), 0.5 mL of 1×10^6 h-TERT cells suspended in modified DMEM, 2.5 mL Type I collagen (First Link Ltd) and 2.5 mL of 0.1*M* sodium hydroxide (Sigma–Aldrich). The gel was vortexed and pipetted into three and incubated overnight (37°C with 5% CO_2). The following day, a needle was used to detach the sides of the gel from the well. Fresh DMEM conditioned media was added and changed weekly. The gels were left to contract for 4 days before use in experiments.

Addition of mNPs within 3D gels

Three mNPs (100, 200, and 500 nm) (Chemicell GmBH) contained a fluorescent tag. Previous evaluation of untagged and tagged NPs has determined no significant difference in cell behavior in terms of viability (up to 72 h) and particle uptake. The 100 and 200 nm sized NPs had a magnetite (Fe_3O_4) iron oxide core whereas, the 500-nm sized NP had a maghemite (Fe_2O_3) iron oxide core. All NP solutions were prepared to a working concentration of 0.1 mg mL^{-1} in modified DMEM. Following fibroblast-mediated gel contraction, gels were transferred to 96-well plates and 75 μL of the mNP solution was added to each gel. Control gels were prepared with 75 μL of modified DMEM only. The gels were incubated (37°C with 5% CO_2) with the mNPs for 1 and 24 h. One plate was subjected to a 280 mT static magnetic field force delivered by FACTOR-96 device (Chemicell), whilst the other plate was incubated without a magnetic field.

Cell viability

Cell viability was assessed after 24-h incubation, the mNP solutions and control solutions were removed and the gels were washed. Each gel was incubated at 37°C for 1 h with a working solution of ethidium homodimer and calcein AM (live/dead staining kit, Invitrogen) (1 μL mL^{-1} in modified DMEM). The solution was removed and the gels were washed before mounting on microscopy slides. Images were taken on a Leitz DMIRB fluorescence microscope at 20× magnification.

Immunofluorescence cytoskeleton F-Actin staining

Following mNP incubation, the gels were washed with 1× phosphate buffered saline (PBS), fixed for 15 min at 37°C, permeabilized for 5 min at 4°C, 1% BSA/1xPBS was added to each well for 5 min at 37°C. F-actin was stained using rhodamine-phalloidin (1:500 in 1% BSA/1xPBS) for 1 h at 37°C. The cells were washed with 0.5% Tween20/1xPBS and mounted onto slides with DAPI (to stain DNA). Images were taken using a Leitz DMIRB fluorescence microscope at 40× magnification.

Scanning electron microscopy (SEM)

After the appropriate incubation period, gels were rinsed twice with 2% sucrose in 0.1*M* sodium cacodylate solution, and then fixed in 6% gluteraldehyde in 0.1*M* sodium cacodylate solution (4°C for 1 h) and then post fixed in 1% osmium tetroxide for 1 h. The gels were washed with distilled water (2 × 10 min), and then stained for 1 h with 0.5% uranyl acetate. The gels were dehydrated by increasing concentrations of ethanol (30, 50, 70, 90, 100, and 100% (dry)) and hexamethyl-disilazane for two 5 minute periods. These gels were analyzed using scanning electron microscopy (Jeol 6400 SEM) at an accelerating voltage of 6 kV at 1500× and 6000× magnification.

Nanoparticle uptake into gels [via inductively coupled plasmas-mass spectrometry (ICP-MS)]

ICP-MS analysis was carried out to determine levels of iron uptaken from the surrounding media into the 3D gel structures. Various groups have used different methods to determine iron concentration in biological samples, however ICP-MS is considered to be the most accurate.[19] Essentially, ICP-MS is a rapid, sensitive analytical tool, which allows the

accurate determination of iron levels with sub ppb detection limits (compared against internal standards). Gels with added NPs were prepared as discussed previously, additionally a further 75 μL of 0.1 mg mL^{-1} NP solution of each NP size was added to wells without any gel. After the appropriate incubation period, samples were processed for ICP-MS as described previously.[17] Briefly, 75 μL of the residing solution was removed and added to 1 mL of distilled water in 50 mL tube. Each well was washed with 100 μL of distilled water and added to an allocated tube. A 1 mL of *aqua regia* was added to each tube and incubated at 70°C overnight. Distilled water was added to each sample tube to give a final volume of 50 mL in preparation for analysis of Fe, along with relevant blank controls, using ICP-MS (THERMO X Series II).

Nanoparticle depth penetration into gels via confocal microscopy

Gels with the addition of NPs were prepared as discussed previously. After the appropriate incubation period, gels were washed twice with 1xPBS and then fixed for 25 min at 37°C. Sequential images were taken at 4-μm intervals to create a z-stack on a Zeiss Axiovert 200M confocal microscope at 20× magnification.

Nanoparticle and cell interaction via histology

To identify mNPs in the cell seeded gels, gel-mNP incubation was performed with each mNP species (100, 200, 500 nm), for 18 h and, following washing in PBS, processed for histology to obtain a cross-sectional view of the gels. Gels were fixed in 4% formaldehyde/1xPBS with 1% sucrose at 37°C for 15 min, submerged in 1 mL permeabilization buffer at 4°C for 15 min and embedded in paraffin wax. Sections of 4 μm thickness were cut from the gel onto polysine coated slides (CellPath, UK) and baked at 60°C overnight. Sections were then de-waxed in xylene for 5 min and rehydrated through graded alcohols (100%, 70%) before rinsing with H_2O for 5 min. Sections were stained with Perls Prussian blue to visualize the mNPs (stains iron) and were dehydrated through graded alcohols (70%, 100%), placed in xylene for 1min, mounted and imaged on a Zeiss Axiovert 25 light microscope at 40× magnification.

RESULTS

Cell viability

The effect of a magnetic field on cell viability and the influence of the three mNP species within gels were assessed via fluorescence microscopy. After 24 h, cell viability was not affected by either the mNP size, location within the gel or the presence of a magnetic field (Figure 1 and Supporting Information).

Fluorescence microscopy: Cells and mNPs

The mNPs have a green fluorescent tag attached to the iron oxide core therefore; they may be easily located within the collagen gel, using fluorescent microscopy. Additionally, the cytoskeleton (actin) of the cells may also be immunofluorescently tagged with a different colored fluorophore (Figure 2). The images showed the smaller the size of the NP produced the greater the amount in the gel. However, there was little dependence with time or magnetic field on NPs presence within the gel, between the 100 and 200 nm sized mNPs. Moreover, all the mNPs in Figure 2 were shown to reside near the cells irrespective of magnetic field or incubation times.

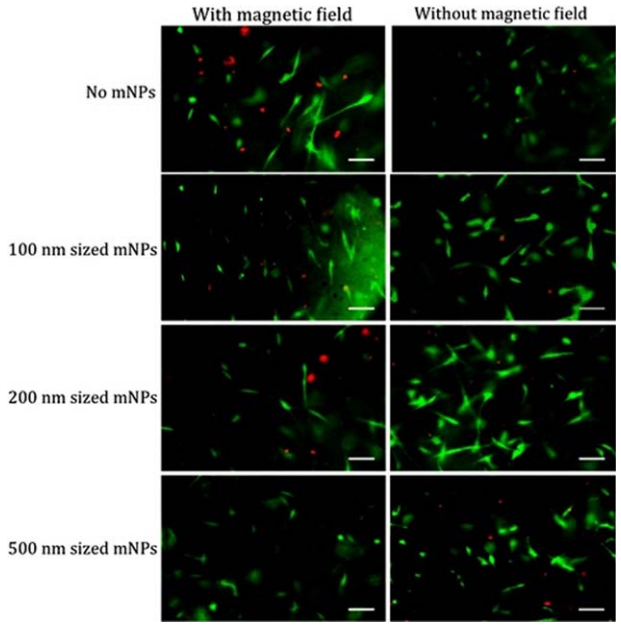

FIGURE 1. Cell viability within collagen gels challenged with different sized mNPs with/without a magnetic field. (Green = alive, red = dead, scale bar = 50 μm) (Magnetic field strength = 280 mT). [Color figure can be viewed in the online issue, which is available at wileyonlinelibrary.com.]

Scanning electron microscopy

SEM was used to observe the surface structure of the gel with the integrated cells and mNPs. Cells were clearly evident across the collagen gel surface, as well as throughout the gel matrix. The mNPs (all sizes) were observed to aggregate with cell contact; however the aggregate size remained smaller than the collagen network pores (Figure 3).

Uptake of mNPs into the collagen gel

The uptake of the mNPs into the gel was measured by calculating the difference of NP concentration within the NP enriched medium, before and after each experimental parameter (1 and 24 h incubation with or without a magnetic field). Initial biological control values were determined for NP medium without gels, to observe the influence of the magnetic field. Whilst there was uptake of all three mNPs into the gel (100, 200, and 500 nm), the uptake was generally both size and time dependent, favoring the smaller mNPs and longer time incubation (Figure 4), and was also enhanced by the presence of a magnetic field.

The highest overall mNP uptake into gels was achieved using the 100 nm sized mNPs incubated for 24 h in the presence of a magnetic field. However, it was noted there were several aberrations to the general uptake trends noted, most notably the high uptake observed by the 200 nm mNPs, in the absence of a magnetic field.

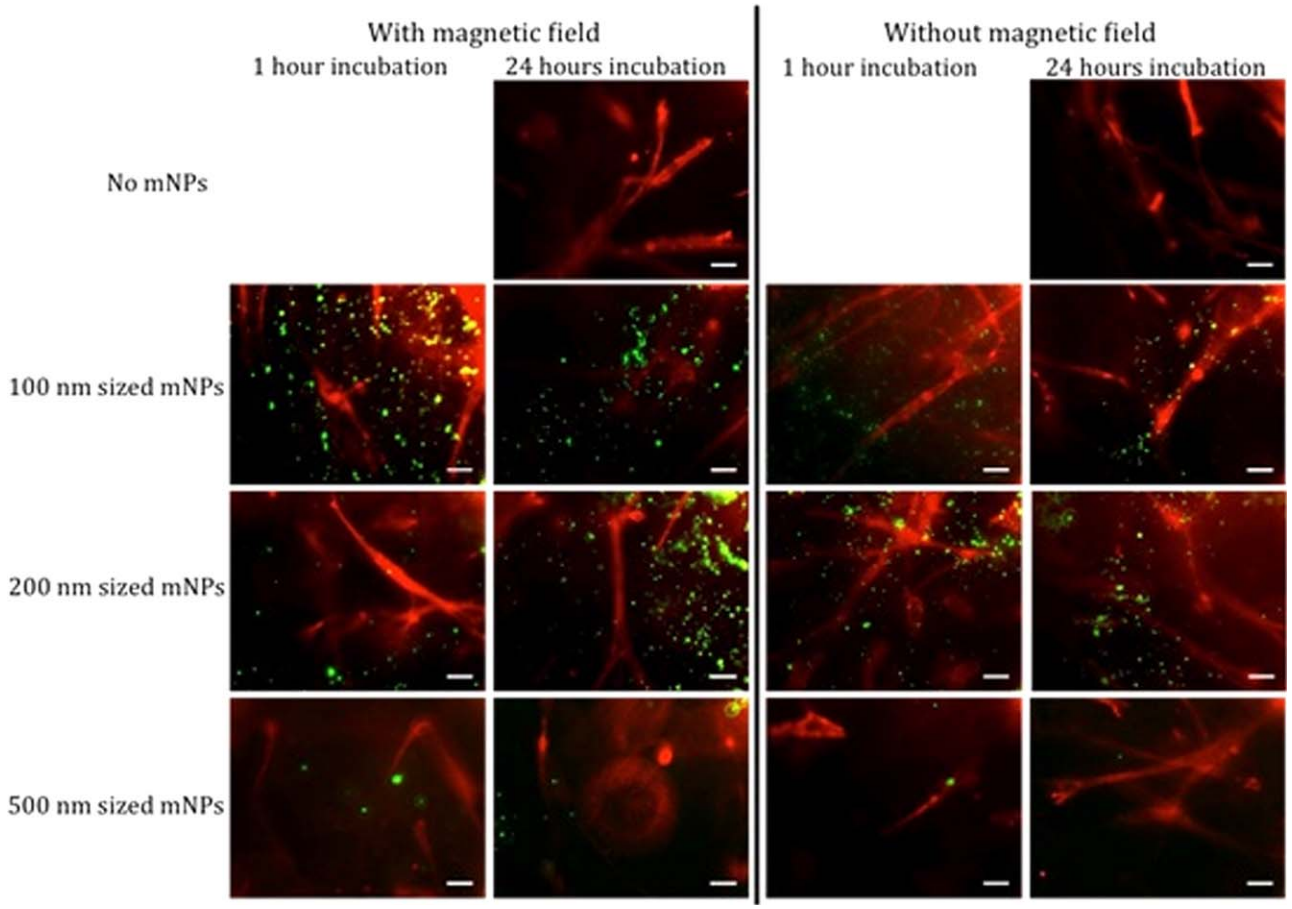

FIGURE 2. Cell proximity to different sized mNPs within collagen gels with/without a magnetic field. (Green = mNPs, red = actin, scale bar = 20 μm). [Color figure can be viewed in the online issue, which is available at wileyonlinelibrary.com.]

Depth of mNP penetration in the collagen gel

The mNPs were fluorescently tagged, so confocal microscopy was used to determine the depth which each mNP penetrated the collagen gel, with or without a magnetic field, over 1 and 24 h (Figure 5).

The results were clearly divided by magnetic field strength, time and mNP size. With regards to magnetic field strength, statistical significant difference was observed with the 100 nm sized mNPs. Furthermore, all the 1-h time points had significantly greater depth penetration compared to the 24-h time points.

The 100 and 200 nm particles behaving similarly, and the 500 nm particles being clearly different. Indeed, with both the 100 and 200 nm particles, the earlier time point indicated the furthest penetration, which was surprising. Furthermore, the magnetic field did not appear to particularly enhance the depth of penetration. The furthest penetration occurred in the presence of a magnetic field, but only after only 1 h and with the medium-sized 200 nm NPs. In general, the 200 nm sized particles denotes higher statistical significance compared to the 100 nm sized particles at both time points with or without a magnetic field.

Conversely, the 500 nm particles demonstrated there was depth penetration dependent upon both time and a magnetic field, with a lowest penetration evident at 1 h without a magnetic field. Furthermore, the 500 nm sized particles had significantly lower depth penetration compared to the 100 and 200 nm sized particles. Error bars denoting the standard deviation were narrow, indicating high precision of the results.

Nanoparticle/cell interaction within the gel

Because of the disperse nature of the cells embedded within the gel, visualizing cellular uptake via transmission electron microscopy proved difficult, therefore Perl's Prussian blue staining was employed. The stain allowed visualization of the cells and iron nanoparticles within the gel structure, therefore allowing verification of cellular uptake (Figures 6 and 7). The top panel in both figures illustrates the top of the gel, with a concentrated layer of cells evident due to cell-mediated contraction. However, the lower panel illustrates slightly further into the gel (~60–100 μm); where cells were stained with Prussian blue, indicating the internalization of NPs (annotated with an arrowhead).

Without a magnetic field present (Figure 6), the 500 nm particles are clearly evident aggregating mainly at the gel/cell surface where they come into contact with the cell layer, however some particles are evident in cells further into the

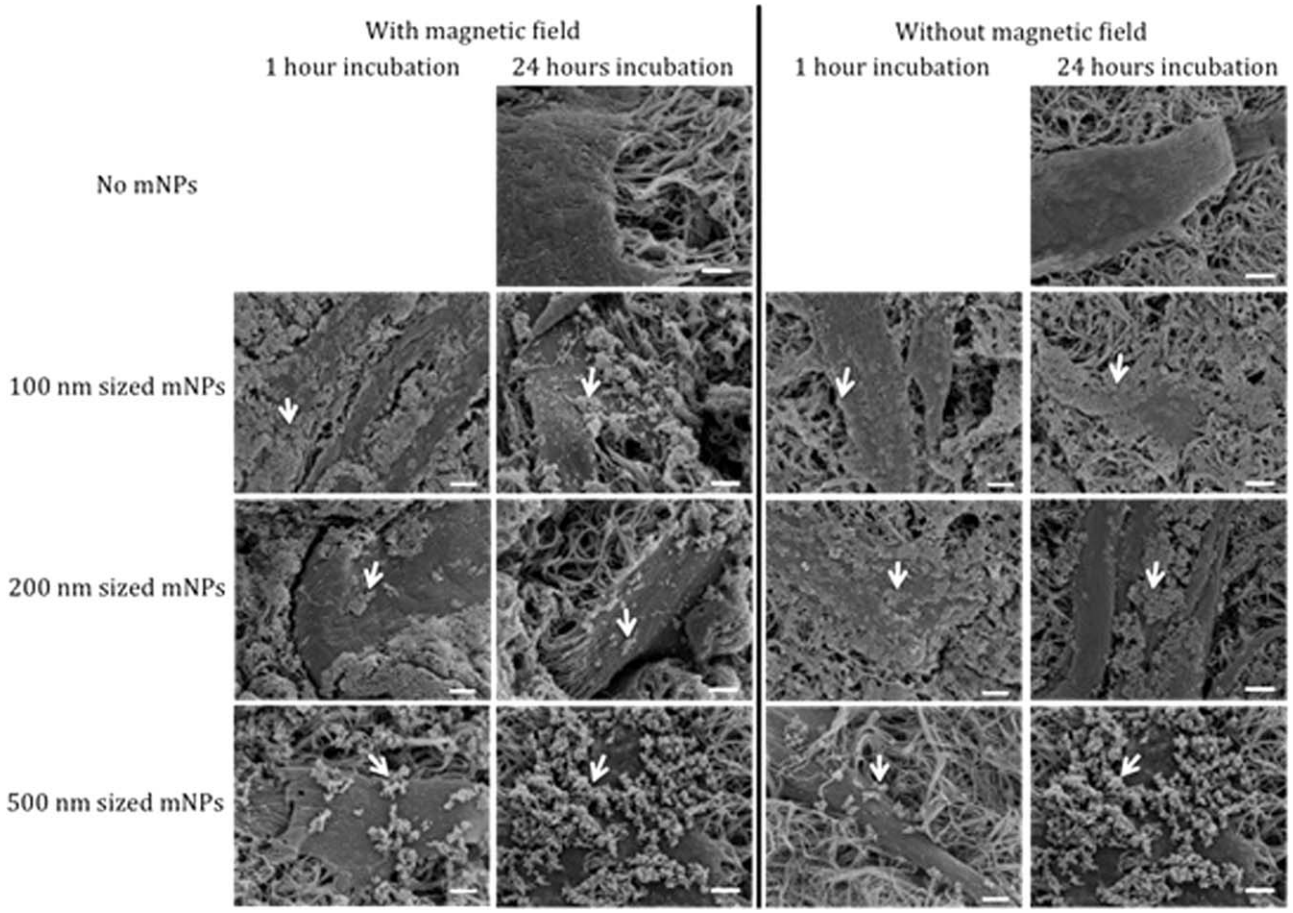

FIGURE 3. SEM images depicting the surface of the collagen gels. Cells were evident on and in the gel matrix as were the mNPs (see white arrows). (Scale bar = 2 μm).

gel (~30–50 μm) with occasional large aggregates free in the collagen network. This supports the confocal and ICP-MS results (Figures 4 and 5, respectively), where fewer 500 nm particles were evident in the gel via fluorescence and also demonstrated a lower uptake into the gel via ICP-MS. Both the 100 and 200 nm particles were clearly apparent in cells in the gel, demonstrating that they are capable of penetrating the gel and being taken up by cells.

With a magnetic field (Figure 7), a clear difference was noted in that both the 100 and 200 nm NPs were also being retained at the cell layer surface of the gel. However, there were still NPs evident within the gel structure.

DISCUSSION AND CONCLUSION

The screening of therapeutic delivery to cells *in vitro,* generally relies on traditional two-dimensional cultures however,

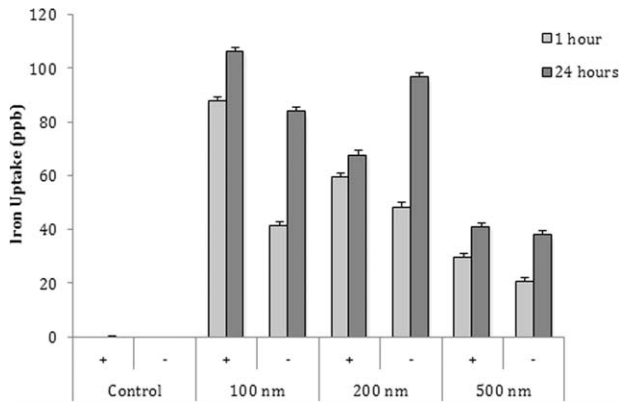

FIGURE 4. Iron uptake into gels as assessed by ICP-MS. Cell seeded gels were challenged with mNPs in the presence or absence of a magnetic field (indicated by + or –, respectively) for either 1 or 24 h.

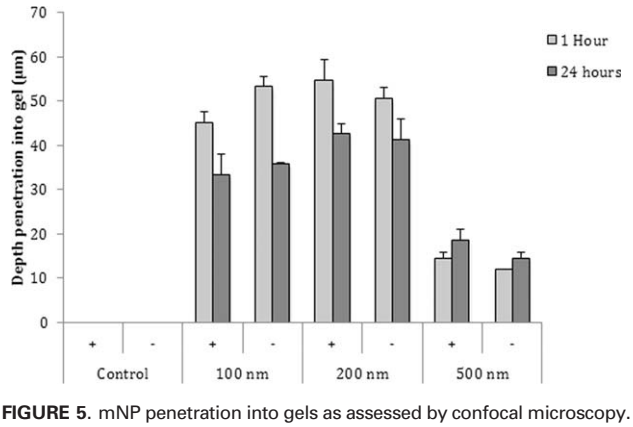

FIGURE 5. mNP penetration into gels as assessed by confocal microscopy. Cell seeded gels were challenged with mNPs in the presence or absence of a magnetic field (indicated by + or –, respectively) for either 1 or 24 h. Results displayed indicate the depth of particle penetration ($n = 3$).

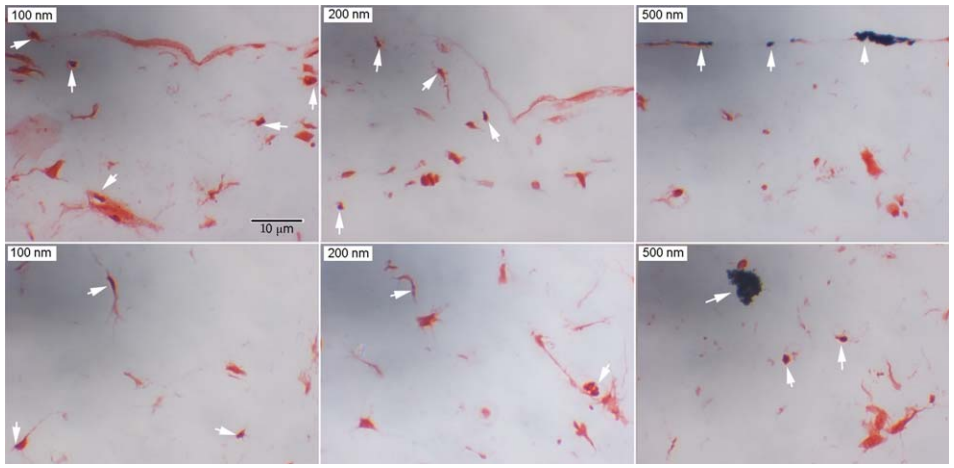

FIGURE 6. mNP uptake into gel and cells as demonstrated by Perls Prussian blue staining in the absence of a magnetic field. (Cells = red, mNPs = blue highlighted by white arrows, scale bar = 10 μm). [Color figure can be viewed in the online issue, which is available at wileyonlinelibrary.com.]

there is a recent drive to assess cell delivery in 3D models, which better reflect the *in vivo* environment. This was recently highlighted by Zhang et al., who investigated DNA delivery into cell cultures in both 2D and 3D (type I collagen matrices), using a range of commercially available transfection reagents.[20] Despite high efficiency in the 2D cultures (generally >80%), there was very little or no efficiency (<1%) for the parallel 3D cultures. This result was attributed to an inability to permeate the collagen matrix. Subsequent experiments utilized mNPs (250 nm) and an external field as a means of delivery, with a slightly greater success rate (~5%). However, the authors surmised the NPs were too large, and were struggling to permeate the collagen matrix. Excellent results were eventually achieved using smaller mNPs (36–56 nm). This article highlighted the importance of NP size when considering utilizing mNPs to facilitate delivery in complex *in vivo* tissues.

This article compared three differently sized mNPs (100, 200, 500 nm) in terms of their ability to (1) to be taken up into a cell-seeded collagen gel matrix. The uptake into and penetration through a collagen gel is reliant on a balance between passive resistive forces in the matrix (including fluid flow) and the induced magnetic force. The results shown in this article indicate the smaller 100 nm mNPs in the presence of a magnetic field exhibit the best initial uptake into the gel. However it was clearly the 200 nm particles that demonstrated the better depth of gel penetration. Furthermore, in the absence of a magnetic field, it was again the 200 nm particles that showed both the highest uptake and subsequent greatest depth penetration. The larger 500 nm particles were by far the lowest on both uptake and depth penetration. This was surprising, as there was an assumption that the smaller 100 nm NPs would prove beneficial in this system. As a collagen gel contracts down due

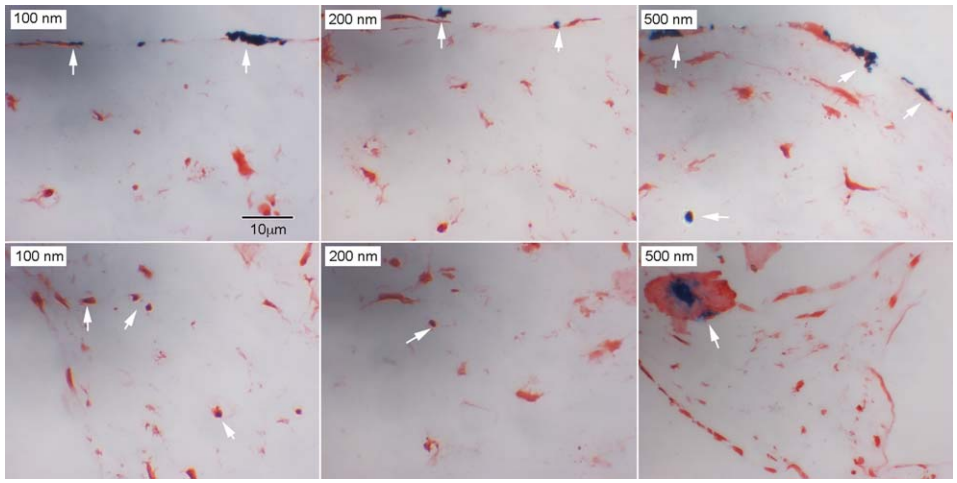

FIGURE 7. mNP uptake into gel and cells as demonstrated by Perls Prussian blue staining in the presence of a magnetic field. (Cells = red, mNPs = blue highlighted by white arrows, scale bar = 10 μm). [Color figure can be viewed in the online issue, which is available at wileyonlinelibrary.com.]

to cell-mediated contraction (typically over an initial period of 5 days from seeding, when it plateaux), the result is a dense connective-tissue equivalent, with a higher density of cells on the outer edge of the gel (due to the contraction). The smaller 100 nm particles exhibited the highest initial uptake into the gel, through this cellular "barrier," indicating smaller sized NPs are either pulled through the cells or between the cells quicker. The subsequent observation that the larger 200 nm particles penetrated and travelled further into the gel structure suggests that this size is more favorable for tissue penetration; however it may also be due to the 100 nm particles being retained at this surface layer of cells. Further histology studies were performed using Perls Prussian blue staining, to identify iron and cells within the gel. As the results showed, without a magnetic field present, the only obvious retention of NPs at the cell surface layer was with the larger 500 nm particles. The smaller 100 and 200 nm particles were evident within cells inside the gel. However, when a magnetic field was present, all three NP sizes were retained at the cell surface layer. This may simply be due to the magnetic force attracting the NPs to the gel surface, causing them to aggregate together (and hence cause retention of the smaller NPs), or it may be that the field increases the chance of cell/NO interaction, and therefore encourages cellular uptake. The smaller NPs were also clearly evident within the gel, so not all were retained.

The movement of mNPs depends directly on a multiple of factors, including the size and shape of the particles, and the characteristics of the suspending medium and strength of the external magnet. Collagen is a viscoelastic protein, and understanding NP movement through the gel system is complex. Previous studies have investigated the movement of mNPs through simple viscous fluids, such as glycerol, studying the movement of particle groups over length scales on interest (e.g., μm and mm), indicating clear movement towards external magnets.[21] Similar studies in fibrin gels, to the extent of using high field strengths (3 T) reporting travel of 10 nm mNPs across distances of 20 mm (in several days).[21]

When considering the use of an external magnetic field, the net motive force of a mNP is governed by electromagnetic theory and Newton's Law, which is determined by the sum of forces acting on the NP, including diffusion, convection, and the magnet.[22] The overall driving force in this case is assumed to be the magnetic force (280 mT), which enable the mNP to overcome the mechanisms, which limits transport, and results in the NP being pulled into the collagen matrix. Therefore, this study would have expected to observe a field dependent increase of mNP uptake into gels and depth of penetration. However, the success of the 200 nm particles to both be taken up and penetrate the gel, particularly in the absence of a magnetic field, indicated the situation was more complex than originally thought.

The pore size and connectivity distribution was obviously a major constraint on NP uptake. The collagen fiber network in the extracellular matrix has been estimated to have gaps ranging from 20 to 130 nm in tumor tissue (a major therapeutic target).[23] Our model varies in this regard due to the addition of cells. The inclusion of cells will change the mechanical properties of the gel (in terms of stiffness) and the density of the gel network (due to cell-mediated gel contraction), so whilst making it a more relevant model with respect to the *in vivo* situation, there will be differences in how a NP can diffuse through our cell-seeded network as opposed to a gel network without cells. These gaps or pores form a physical barrier to passive NP transport (i.e., without a magnetic field). The pores evident in this *in vitro* model appear to be large ($\sim$30–600 nm) and do not appear to sterically hinder the NP diffusion (Figures 6 and 7).

In addition to the physical barrier described above, NP interactions with the surrounding environment, including soluble proteins, carbohydrates, and other mNPs may also lead to restriction of particle transport. A certain degree of mNP adhesion to such structures was expected, and the SEM images presented in this study show, a level of aggregation which was clearly evident for all three mNP sizes, particularly at the cell surface. However, this aggregation did not appear to decrease the particle motility and it may even have increased the susceptibility to the magnetic force.

This article has shown there are several factors affecting mNP penetration and up take, including collagen pore size and subsequent interactions with the surrounding environment. The use of a 3D *in vitro* tissue equivalent model, showed large mNPs (500 nm) are not effectively taken up or able to penetrate the collagen matrix compared to smaller mNPs ($\leq$200 nm). However, the study also showed mNP uptake improved with time, regardless of size or in the presence magnetic field.

REFERENCES

1. Liu W-T. Nanoparticles and their biological and environmental applications. J Biosci Bioeng 2006;102:1–7.
2. Wilson CG, Sisco PN, Gadala-Maria FA, Murphy CJ, Goldsmith EC. Polyelectrolyte-coated gold nanorods and their interactions with type I collagen. Biomaterials 2009;30:5639–5648.
3. Sun C, Lee JSH, Zhang M. Magnetic nanoparticles in MR imaging and drug delivery. Adv Drug Deliv Rev 2008;60:1252–1265.
4. Chen GD, Alberts CJ, Rodriguez W, Toner M. Concentration and purification of human immunodeficiency virus Type 1 virions by microfluidic separation of superparamagnetic nanoparticles. Anal Chem 2009;82:723–728.
5. Dejardin T, de la Fuente J, del Pino P, Furlani EP, Mullin M, Smith CA, Berry CC. Influence of both a static magnetic field and penetratin on magnetic nanoparticle delivery into fibroblasts. Nanomedicine 2011;6:1719–1731.
6. Berry CC. Progress in functionalization of magnetic nanoparticles for applications in biomedicine. J Phys D Appl Phys 2009;42:224003.
7. Dobson J. Magnetic nanoparticles for drug delivery. Drug Dev Res 2006;67:55–60.
8. Chomoucka J, Drbohlavova J, Huska D, Adam V, Kizek R, Hubalek J. Magnetic nanoparticles and targeted drug delivering. Pharmacol Res 2010;62:144–149.
9. Medeiros SF, Santos AM, Fessi H, Elaissari A. Stimuli-responsive magnetic particles for biomedical applications. Int J Pharm 2011; 403:139–161.
10. Sahay G, Alakhova DY, Kabanov AV. Endocytosis of nanomedicines. J Controlled Release 2010;145:182–195.
11. Lakadamyali M, Rust MJ, Zhuang X. Endocytosis of influenza viruses. Microbes Infect 2004;6:929–936.
12. Plank C, Scherer F, Schillinger U, Bergemann C, Anton M. Magnetofection: Enhancing and targeting gene delivery with superparamagnetic nanoparticles and magnetic fields. J Liposome Res 2003;13:29–32.

13. Smith C-AM, Fuente JdI, Pelaz B, Furlani EP, Mullin M, Berry CC. The effect of static magnetic fields and tat peptides on cellular and nuclear uptake of magnetic nanoparticles. Biomaterials 2010;31:4392–4400.
14. Goodman TT, Ng CP, Pun SH. 3-D tissue culture systems for the evaluation and optimization of nanoparticle-based drug carriers. Bioconjug Chem 2008;19:1951–1959.
15. Mondalek FG, Zhang YY, Kropp B, Kopke RD, Ge X, Jackson RL, Dormer KJ. The permeability of SPION over an artificial three-layer membrane is enhanced by external magnetic field. J Nanobiotechnol 2006;4:4.
16. Gao X, Grady BP, Dormer KJ, Kopke RD, Wang Y, Chen K. Magnetic assisted transport of PLGA nanoparticles through a human round window membrane model. J Nanotechnol Eng Med 2010; 1:031010–031010. Available at: http://nanoengineeringmedical.asmedigitalcollection. asme.org/article.aspx?articleid=1452330.
17. Child HW, del Pino PA, De La Fuente JM, Hursthouse AS, Stirling D, Mullen M, McPhee GM, Nixon C, Jayawarna V, Berry CC. Working together: The combined application of a magnetic field and penetratin for the delivery of magnetic nanoparticles to cells in 3D. ACS Nano 2011;5:7910–7919.
18. Sensenig R, Sapir Y, MacDonald C, Cohen S, Polyak B. Magnetic nanoparticle-based approaches to locally target therapy and enhance tissue regeneration in vivo. Nanomedicine (Lond) 2012;7: 1425–1442.
19. Rad AM, Janic B, Iskander A, Soltanian-Zadeh H, Arbab AS. Measurement of quantity of iron in magnetically labeled cells: Comparison among different UV/VIS spectrometric methods. BioTechniques 2007;43:627–636.
20. Zhang H, Lee M-Y, Hogg MG, Dordick JS, Sharfstein ST. Gene delivery in three-dimensional cell cultures by superparamagnetic nanoparticles. ACS Nano 2010;4:4733–4743.
21. Kalambur VS. Biotransport of Iron Oxide Magnetic Nanoparticles for Biomedical Applications. Ann Arbor: University of Minnesota; 2007. pp 159.
22. Kuhn S, Hallahan D, Giorgio T. Characterization of superparamagnetic nanoparticle interactions with extracellular matrix in an in vitro system. Ann Biomed Eng 2006;34:51–58.
23. Seisenberger G, Ried MU, Endreß T, Büning H, Hallek M, Bräuchle C. Real-time single-molecule imaging of the infection pathway of an adeno-associated virus. Science 2001;294:1929–1932.